

Tuning the Photocatalytic Activity of Nanocrystalline Titania by Phase Composition Control and Nitrogen Doping, Using Different Sources of Nitrogen

Nejc Rozman,¹ Luka Škrlep,¹ Miran Gaberšček² and Andrijana Sever Škapin^{1,*}

¹ Slovenian National Building and Civil Engineering Institute, Dimičeva 12, Ljubljana, Slovenia

² National Institute of Chemistry, Hajdrihova 19, Ljubljana, Slovenia

* Corresponding author: E-mail: andrijana.skapin@zag.si

Received: 23-12-2013

Dedicated to the memory of Prof. Dr. Marija Kosec.

Abstract

Titania nanoparticles were synthesized by employing the hydrothermal method and using TiOSO_4 as a titanium source. By varying pH between 0.5 and 1.0 and adding isopropanol to the hydrothermal reaction mixture, different mixtures of anatase, rutile, and brookite were obtained. The samples were also doped with nitrogen at different N concentrations using, respectively, urea, ammonium nitrate, and tripropylamine as nitrogen sources. The samples were characterized by X-ray powder diffraction, field emission scanning electron microscopy, infrared spectroscopy, UV-Vis diffuse reflectance spectroscopy and according to their specific surface area. Additionally, their photocatalytic activity was measured in a gas-solid reactor system. The results show that low pH favours rutile formation, whereas a higher pH yields mixed phase titania polymorphs. Isopropanol addition also favours rutile formation, and boosted the photocatalytic activity of the resulted particles. Contrary to most data in the literature, rutile turned out to be the more active phase in the present investigation. Nitrogen doping, on the other hand, did not contribute to higher photocatalytic activity, but was rather detrimental to it.

Keywords: Titania, rutile, hydrothermal synthesis, photocatalysis, nitrogen doping

1. Introduction

Titanium dioxide is a well-established industrial product, which is mostly used as a white pigment. Ever since the discovery of its photocatalytic potential by Honda and Fujishima,¹ this special property of an otherwise common material has been in the forefront of materials research. Since TiO_2 is a wide band gap semiconductor, its photocatalytic activity is limited to UV and near-UV light, which constitutes only a small part of the solar spectrum.^{2,3} The proper tailoring of TiO_2 properties, using economically feasible reagents and procedures, is crucial if photocatalytic TiO_2 is to become a widely used material.^{2,4,5}

In order for photocatalysis to become more efficient, a wider spectrum of solar energy should be utilized, e.g. the visible part of the spectrum, as well as UV, should be exploited. In order to achieve this goal, band gap modification through the doping and co-doping of various hete-

roatoms in the crystal lattice of titania has been proposed.^{2,4,6–9} However, doping is a complex process that may also influence other important parameters such as crystallite size and morphology, the charge carrier recombination rate, and the charge transfer rate. All of these factors have an influence on the photocatalytic degradation of pollutants. The influence of doping on photocatalysis is not always beneficial, and can even be detrimental. Choosing dopants and co-dopants and determining their optimal concentration leads to a combinatorial explosion of material modification possibilities.^{2,4,6,10–12}

According to the literature, one of the most favourable dopants is nitrogen.^{3,10,11,13–18} Many reports have found that nitrogen doping effectively reduces band gap energy and therefore promotes visible light photocatalysis. The mechanism of band gap reduction is still controversial and several hypotheses have been proposed to explain N-doped TiO_2 photocatalytic behaviour exposed to visible light.^{3,13,14} Different sources of nitrogen create specific chemical envi-

ronments and can yield somewhat different results concerning the dopant position, either substitutional or interstitial, and consequently the band gap reduction, size, and morphology of TiO_2 nanoparticles, all of which have significant effect on the photocatalytic performance of TiO_2 .^{10,15,19}

TiO_2 synthesis may be performed by means of different routes and by using various reagents. Among wet chemical methods the most notable are sol-gel syntheses, which usually employ titanium alkoxides as precursors. Hydro- and solvothermal syntheses are another set of commonly used procedures. Although titanium alkoxides are the most commonly used reagents, titanium tetrachloride, titanyl nitrate and titanyl sulphate can also be used.^{4,20–25} Our work was focused on the latter reagent, employing hydrothermal synthesis to obtain the product.

The focus of the first part of the study was on the dependence of titania phase composition on pH at the very low end of the scale (the pH was varied between 0.5 and 1.0). Additionally, the influence of isopropanol addition on phase composition is discussed. The effect of the anatase:rutile ratio in the obtained titania products on the latter's photocatalytic activity is systematically studied and commented upon.

In the second part of the study, titania was doped with nitrogen using different sources (ammonium nitrate, urea, and tripropylamine) in different concentrations, while also varying the pH of the samples – taking into account the knowledge collected in the first part of the work. In all cases isopropanol was added to the samples.

2. Experimental

2.1. Synthesis

Titanium oxysulphate, TiOSO_4 , (Sigma Aldrich, 29% \geq as TiO_2) was dissolved in distilled water while stirring, containing 15 wt.% of reagent powder in the solution. The mixture was stirred magnetically until it turned into a co-

lourless solution. The ammonium hydroxide solution, with an ammonia content of 25% (Sigma Aldrich, NH_4OH) was diluted to an ammonia content of 10%. The ammonia solution was added instantaneously to a titanium oxysulphate solution under vigorous stirring so that the pH value of the precipitated gel reached 8. The reaction took place in a beaker. The obtained amorphous gel was then filtered and rinsed several times using distilled water, so that no residual sulphate or ammonium ions remained. After rinsing, water was added to the gel, so that the TiO_2 content was 5 wt.%. The dispersed gel was then mixed in a dissolver at 4500 rpm for at least 30 minutes. 28 grams of the obtained mixture was transferred to a standard Teflon-lined stainless steel autoclave with total volume of 40 mL, where its pH was adjusted using nitric acid (HNO_3 , 65%, Sigma Aldrich). The pH of the samples was set at either 0.5, 0.7 or 1.0. Teflon-lined autoclaves were chosen because this material is known to be inert even in very low pH conditions.

The undoped samples were either i) immediately enclosed in the Teflon autoclave or ii) enclosed in the autoclave after addition of an appropriate amount of isopropanol. In both cases autoclave was then put into a pre-heated oven at 200 °C for 18 hours (see Figure 1). The filling level in the autoclave was 80%.

For the doped samples, an appropriate amount of dopant precursor was added to the mixture in the autoclave, the pH of which was adjusted prior to dopant precursor addition. The mixture was then stirred for at least 15 minutes. Just before enclosing the autoclaves, 0.5 mL of isopropanol was added. The mixture was then sealed in the autoclaves and put into a pre-heated oven at 200 °C for 18 hours. To ensure similar conditions, the filling level of all the autoclaves reached 80%.

After the heating phase the autoclaves were taken out of the oven and left to cool at room temperature. The obtained product was filtered, rinsed, and dried under ambient conditions.

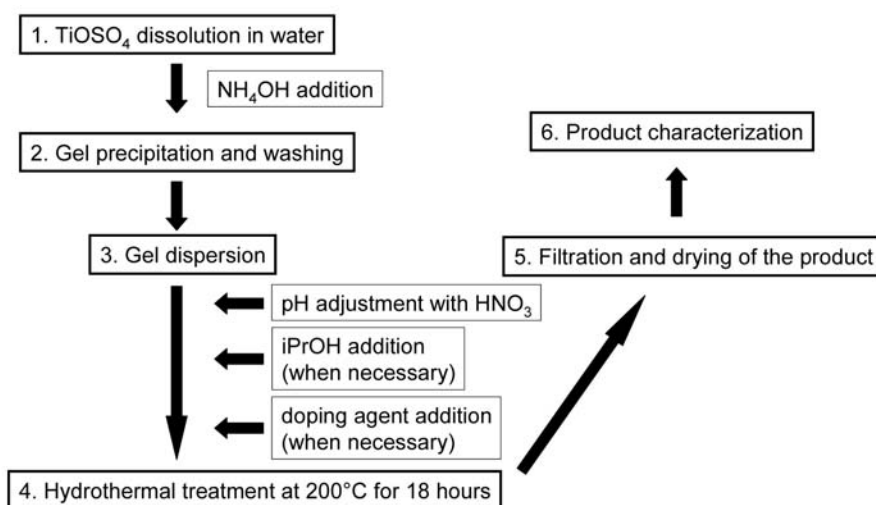


Figure 1. Schematic presentation of the synthesis procedure.

The dopants were ammonium nitrate (NH_4NO_3), urea ($\text{CO}(\text{NH}_2)_2$) and tripropylamine (TPA – $(\text{CH}_3\text{CH}_2\text{CH}_2)_3\text{N}$). An appropriate amount of ammonium nitrate (0.21 g) or urea (0.28 g) was dissolved in 10 mL of distilled water; 1 mL of these solutions corresponds to the dopant concentration of 1 at.% of nitrogen in TiO_2 . The volume of dopant solution added to the synthesis mixture was 0.5, 1.0 or 2.0 mL which correlates to 0.5, 1.0 or 2.0 at.% of nitrogen doping, respectively (see Figure 1).

2. 2. Product Characterization

Structural characterization of the samples was performed by X-ray diffraction (XRD) using D4 Endeavor, Bruker AXS with $\text{K}\alpha$ Cu as the radiation source ($\lambda = 0.154$ nm) and Sol-X as an energy dispersive detector. The fractions of the anatase and rutile phases were calculated using the Spurr equation²⁶:

$$x_a(\text{wt}\%) = \frac{100}{1 + 1,265 \frac{I_r}{I_a}} \quad (1)$$

where x_a is wt.% of anatase in the sample, I_r represents the rutile (110) peak at $2\theta = 27.4^\circ$, and I_a represents the anatase (101) peak at $2\theta = 25.3^\circ$. The fractions of the phases in the three-phased samples (rutile-anatase-brookite) were estimated by using the following equation:

$$x_i = \frac{I_i}{I_a + \frac{I_b}{0.9} + I_r} \quad (2)$$

where x_i represents the wt.% of phase i (either anatase, rutile or brookite), I_i represents the intensity of this phase, and I_a , I_b and I_r represent, respectively, the intensities of anatase, at 25.3° , brookite, at 30.8° , and rutile, at 27.4° , representing the (101), (110), and (121) plane, respectively. In the case of anatase and rutile the highest reflections were taken into account whereas in the case of brookite the second highest reflection was used since its highest intensity reflection at 25.3° overlapped with the anatase reflection. The second highest reflection intensity at 30.8° was therefore used in the calculations, divided by the correction factor of relative intensity compared to the highest intensity at 25.3° , the value of which was 0.9. In the calculations of the fractions of the three polymorphs the possible presence of an amorphous phase was neglected.

The BET surface area was measured by a surface area analyser via nitrogen adsorption-desorption isotherms at liquid nitrogen temperature using a Micrometrics ASAP 2020 instrument.

The size and morphology of the samples was determined using a Zeiss ULTRA plus field emission scanning electron microscope (FE-SEM).

Diffuse reflectance spectroscopy of the samples was performed on a Shimadzu 3600 UV-VIS-NIR spectrophotometer with an ISR-3100 integrating sphere attachment. Barium sulphate was used as a standard. The samples were prepared for measurement by piling a small amount on a layer of barium sulphate powder, after which the sample powder was spread into a thin uniform layer using a glass rod.

FT-IR spectroscopic analysis of samples was performed on a Perkin Elmer Spectrum 100 FT-IR spectrophotometer. A small amount of the sample was ground together with KBr, and the resulting powder was pressed into a

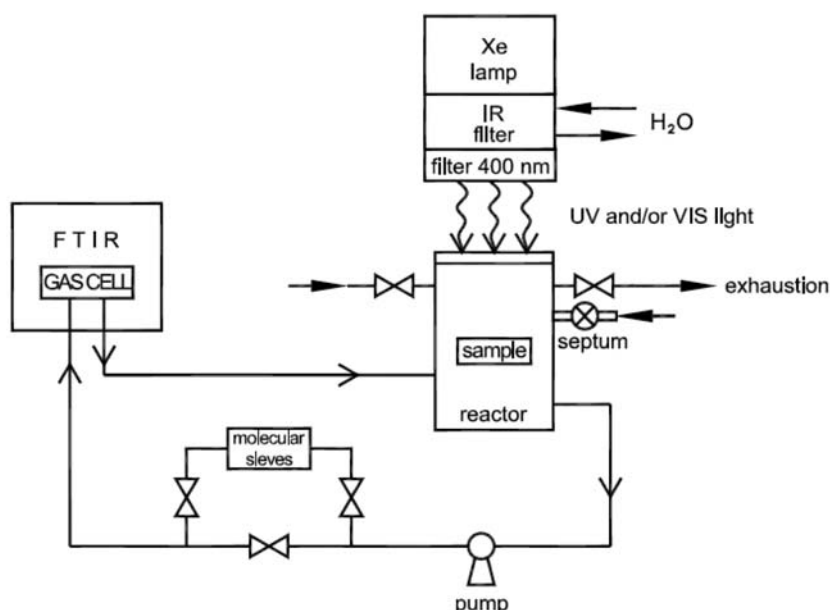
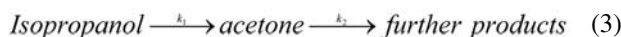


Figure 2. Schematic representation of the gas-solid reactor system.

pellet. The pellet was put into the spectrometer and its spectrum measured.

Photocatalytic activity measurements were performed in a sealed gas-solid reactor utilizing FT-IR spectroscopy on a Spectrum BX model Perkin Elmer spectrometer (see Fig. 2). The method has been described in detail elsewhere.²⁷ The model pollutant was isopropanol. Isopropanol oxidizes over the lit sample into acetone, and this acetone oxidizes into other products. The samples were prepared by milling 50 mg of the sample and uniformly distributing it in a standard petri dish with a diameter of 60 mm.



The first reaction of isopropanol oxidation is fast compared to subsequent reactions, and is usually considered to be a zeroth order reaction. The second step can be assumed to be the first order reaction. Taking into account these two assumptions, the equation for the time dependence of acetone concentration is as follows:

$$C_{\text{acet}}(t)(\text{zero}) = \frac{k_1}{k_2} (1 - e^{-k_2 t}) \quad (4)$$

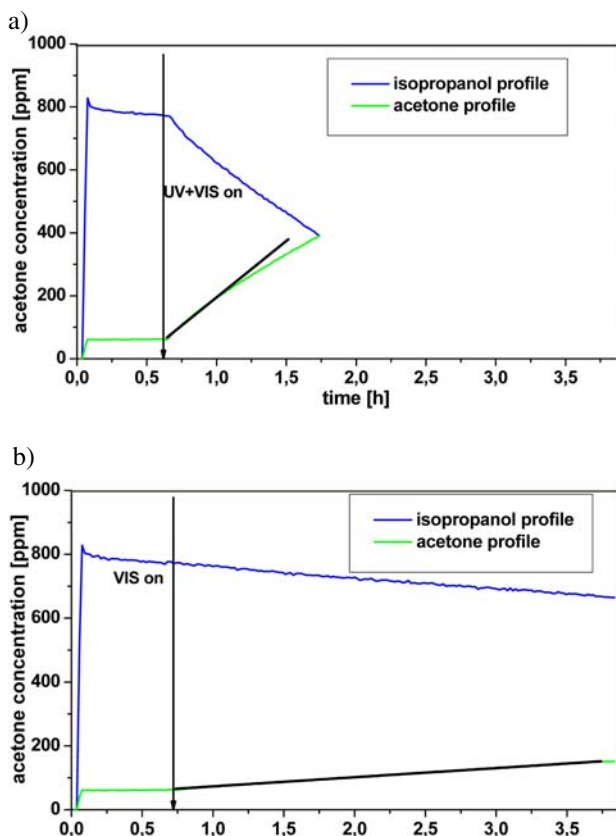


Figure 3. Typical isopropanol (blue) and acetone (green) concentration profiles for the determination of photocatalytic activity: (a) P25 profiles under UV+VIS illumination; (b) P25 profiles under VIS illumination (a filter was used at 400 nm).

The evaluation of photocatalytic activity is based on acetone formation kinetics and given in ppm/h. According to equation (4), the acetone curve would exhibit a peak (i.e. a maximum concentration) at a certain time. However, since $k_1 \gg k_2$ a linear fit of the initial acetone formation kinetics curve can still be made, yielding quite reliable results for photocatalytic activity (see Fig. 3). In order to ensure repeatability of results, temperature and relative humidity were kept at $25 \pm 3^\circ\text{C}$ and $22 \pm 3\%$, respectively. Evonik P25 was also measured regularly in order to ensure the reliability of the method. The results of the prepared samples are also given in terms of the P25 coefficient, i.e. the sample's photocatalytic activity result was divided by the measurement result for the P25 photocatalytic activity, and the obtained number is the P25 coefficient.

The light source for the photocatalytic activity measurements was a 300 W Xe lamp (Newport Oriel Instrument, USA), with an infrared filter. The lamp imitates the solar spectrum and emits both ultraviolet (UV) and visible light (VIS). The results of measurements in UV indicated that the whole spectrum of the light was used, i.e. VIS plus UV, whereas the VIS measurements indicated that a filter was used. This filter cuts out any light under 400 nm, so that in this case the samples were irradiated solely by visible light. In this study, the radiance intensity on the sample was 40 W/m^2 .

3. Results and Discussion

3.1. Dependence of Product Properties on pH and the Addition of Isopropanol

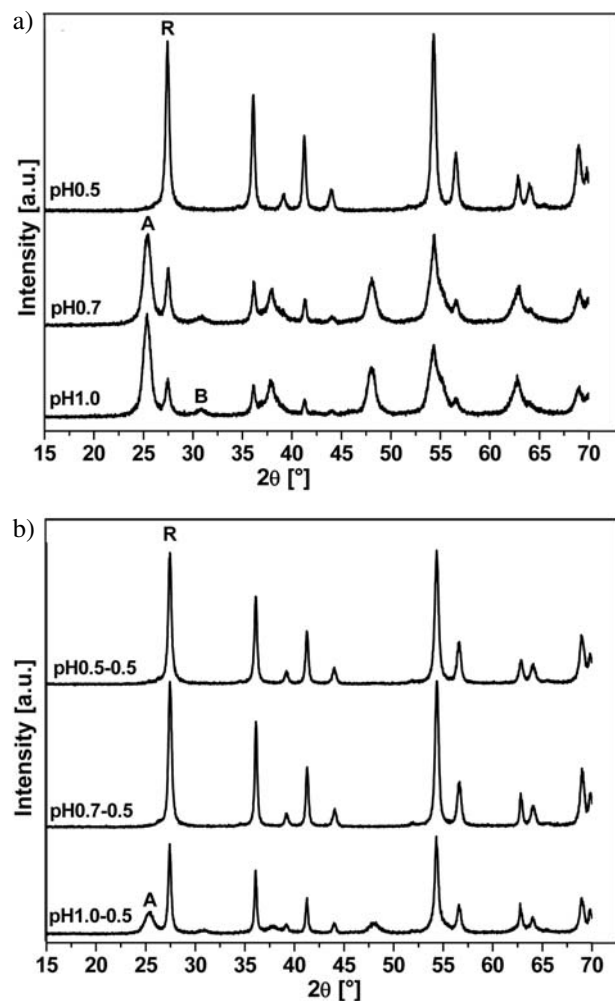
The main properties of titania products as functions of pH and isopropanol addition are shown in Table 1.

The pH of the prepared samples was 0.5, 0.7 and 1.0. As can be seen from Figure 4, where the XRD results are shown, a low pH favours the formation of rutile. The sample pH0.5 showed a distinct reflection at 27.6° , which is characteristic for rutile, and no reflection at 25.5° . The samples pH0.7 and pH1.0 also showed a reflection at 27.6° , although a less pronounced one. These two samples, however, showed another reflection at 25.5° , which is characteristic for samples containing anatase. Another reflection with a low intensity at 32° indicates that the samples pH0.7 and pH1.0 contained a small fraction of the brookite phase. It can therefore be concluded that low pH, in our case a pH value of 0.5, favours rutile formation, whereas higher pH values favour anatase formation with a small fraction of brookite. There is an indication that the higher the pH value the higher is the anatase:rutile ratio. This was also found by Yang et al.²⁸ and Xu et al.²⁹

Structural analysis of the samples with isopropanol addition showed a similar trend, i.e. that low pH values favours rutile formation. The samples pH0.5–0.5 and pH0.7–0.5 contained the rutile phase only, whereas the

Table 1. The results of the samples with varying pH with and without the addition of isopropanol

Sample	pH	iPrOH [mL]	BET SSA [m ² /g]	Anatase [wt.%]	Rutile [wt.%]	Brookite [wt.%]	VIS activity [ppm/h]	UV+VIS activity [ppm/h]
pH0.5	0.5	/	43	0	100	0	70	970
pH0.7	0.7	/	119	57	36	7	10	310
pH1.0	1.0	/	117	66	25	9	9	340
pH0.5–0.5	0.5	0.5	54	0	100	0	95	1150
pH0.7–0.5	0.7	0.5	58	0	100	0	85	1250
pH1.0–0.5	1.0	0.5	100	20	77	3	60	970

**Figure 4.** XRD diffractograms of (a) samples with varying pH without isopropanol, and (b) samples with varying pH with added isopropanol.

sample pH1.0–0.5 contained a certain quantity of the anatase phase. Isopropanol addition seems to favour rutile formation, since pure rutile can be obtained at a higher pH (compare the samples pH0.7 and pH0.7–0.5). For example, the sample pH1.0–0.5 contains a much higher rutile percentage than sample pH1.0. A similar finding was made by Yan et al.³⁰ In their experiments a mixture of

water and ethanol in the hydrothermal reaction mixture yielded a higher percentage of the rutile phase than the reaction mixture of water without ethanol.

Comparing the FE-SEM images (Figures 5a–c) and the BET specific surface area values (Table 1), it is possible to confirm that anatase particles are spherical in shape, with a diameter of 10–15 nm (Figures 5a–c), rutile crystallizes in the form of elongated nanorods, about 50–150 nm in length and 30–60 nm in width, as can be seen from the FE-SEM image in Figure 5d. The anatase containing samples (pH0.7, pH1.0 and pH1.0–0.5) have a significantly higher specific surface area than those composed entirely of rutile. Despite the fact that photocatalysis is a surface phenomenon, where one might expect higher surface area samples to have better photocatalytic activity, it was found that was not the case with our samples. It is important to bear in mind that photocatalysis is a complex phenomenon, which depends on many factors, not just specific surface area. Both sample pH0.7 and sample pH1.0 have significantly higher specific surface area than sample pH0.5, but their photocatalytic activity in VIS is lower by a factor of 7 or more. The anatase containing samples fared somewhat better under UV+VIS irradiation, but their activity was much lower than that of the sample pH0.5, which contains only rutile (see Table 1). It should be noted that photocatalytic activity depends on many factors, among which the model pollutant used is one. The obtained values are specific for isopropanol oxidation and acetone formation, whereas they may be different if another pollutant was used.

In the case of some of the samples a small amount of isopropanol was added before the hydrothermal treatment. Isopropanol addition had two effects. Firstly it influenced phase composition. This effect can only be observed by comparing samples pH0.7 and pH1.0 with samples pH0.7–0.5 and pH1.0–0.5. Sample pH0.7–0.5 was composed entirely of rutile crystallites, whereas sample pH1.0–0.5 still contained the anatase phase, but less of it. Secondly, isopropanol addition also had an effect on the specific surface area of rutile. Comparing the samples pH0.5 and pH0.5–0.5, a somewhat larger specific surface area can be observed in the case of the latter sample (54 m²/g vs. 43 m²/g). Isopropanol also had a significant effect on photocatalytic activity. This can be explained by

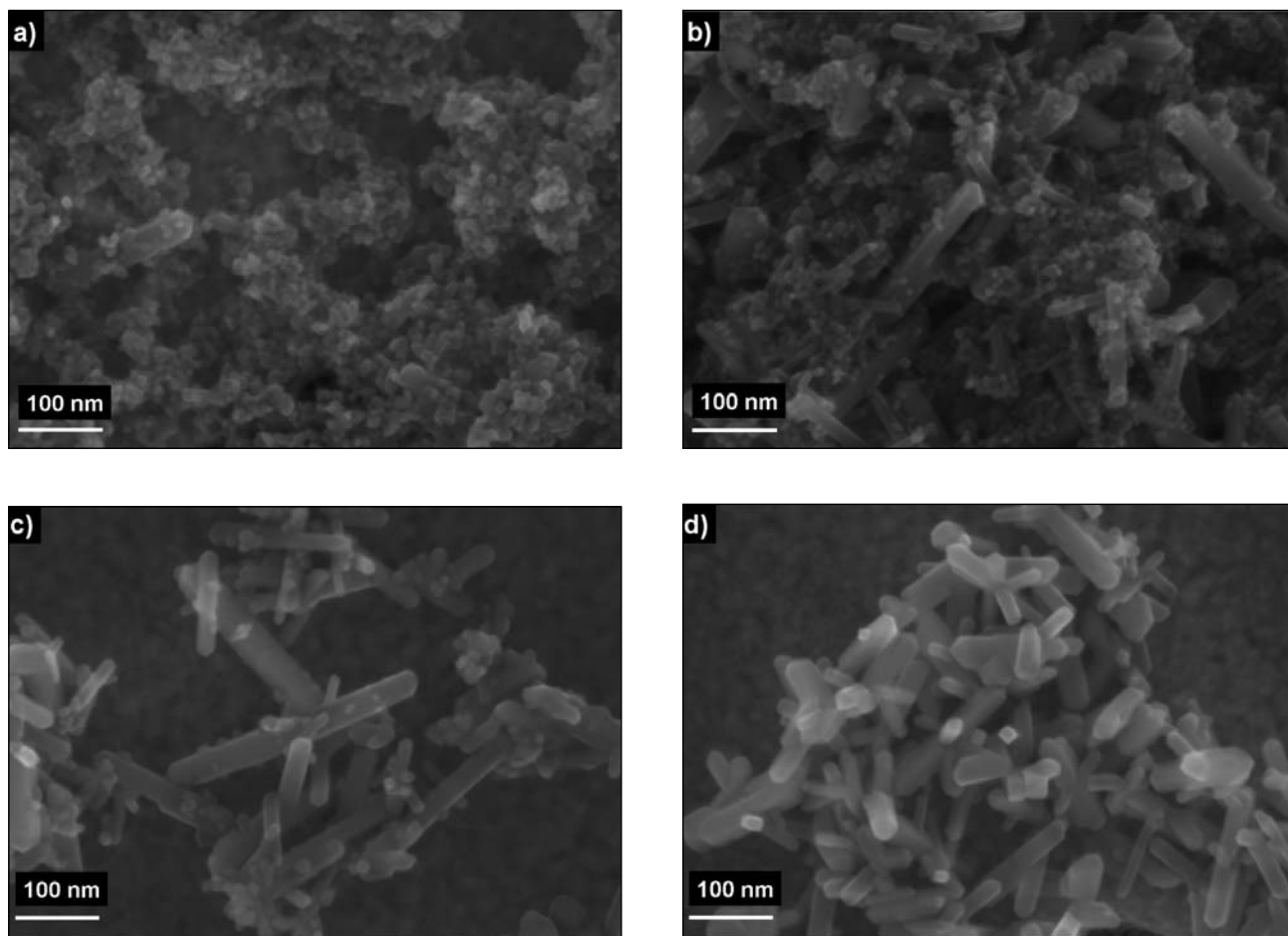


Figure 5. FE-SEM images of samples containing different anatase:rutile phase ratios (a) pH1.0, 25 wt.% rutile, (b) pH1.0–0.5, 77 wt.% rutile, (c) pH0.5–1% NH_4NO_3 , 94 wt.% rutile, and (d) pH0.5–0.5, 100 wt.% rutile.

the higher rutile content, as is the case of samples pH0.7–0.5 and pH1.0–0.5. The rutile phase has already been shown to be more active. However, sample pH0.5–0.5 also had a somewhat higher photocatalytic activity than sample pH0.5, despite the fact that both samples contain only a rutile phase. This may be explained by the somewhat larger specific surface area of sample pH0.5–0.5. Wang³¹ also found that introducing alcohol into the hydrothermal reaction mixture resulted in a higher specific surface area of the titania, although his product was composed of anatase particles.

By comparing the undoped samples with P25, it can be seen that the photocatalytic activity, under VIS irradiation, of the samples without isopropanol was much lower in the anatase-containing samples (pH0.7 and pH1.0), whereas the activity of a rutile phase containing sample, pH0.5, is almost twice as high as that of P25 (Figure 6a). A similar finding can be made in the case of the synthesized samples under UV+VIS irradiation (Figure 6b). The anatase-containing samples have a much lower activity than P25. Sample pH0.5 stands out, since its activity is comparable to that of P25.

As has already been mentioned, those samples to which isopropanol was added before hydrothermal treatment showed, in general, a higher photocatalytic activity. All of them were more active than P25, both under VIS irradiation alone, and under UV+VIS irradiation. The differences in activity under VIS irradiation are relatively large and the sample prepared at pH 0.5 is the most active even in this group (Figure 6c). The difference in activity is much less noticeable under UV+VIS irradiation (Figure 6d). All the samples were more active than P25. However, under UV+VIS irradiation, sample pH0.7–0.5 had the highest photocatalytic activity. Isopropanol addition to the reaction mixture before hydrothermal treatment seems to boost the photocatalytic activity. Since isopropanol addition had a favourable effect on photocatalytic activity, 0.5 mL of isopropanol was added to all the doped samples.

3. 2. Properties of the Nitrogen Doped Samples

In the second part of the experiments, different sources of nitrogen were used for doping the TiO_2 . Nitrogen doping has been widely considered as a promising way of

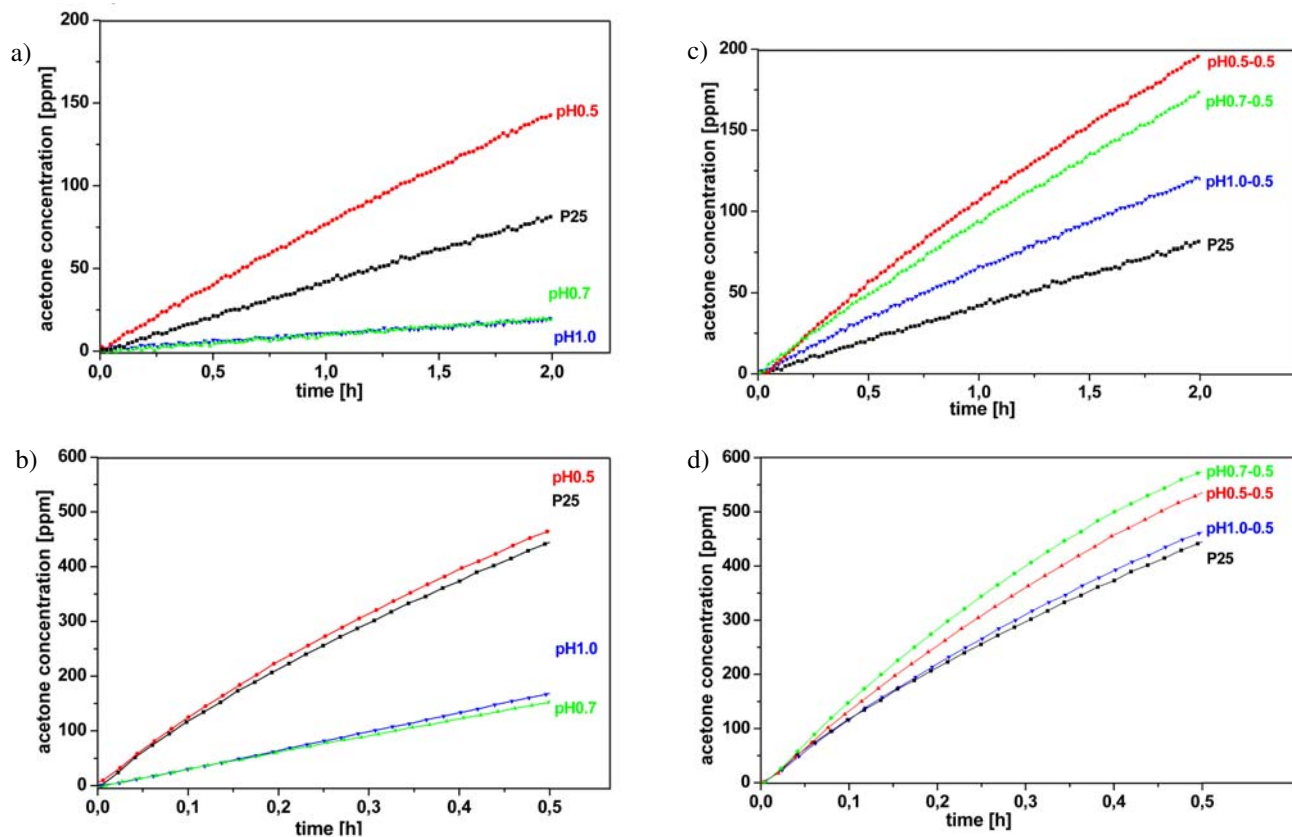


Figure 6. Acetone formation kinetics, from which the photocatalytic activity was calculated (see section 2.2), (a) samples pH0.5, pH0.7, pH1.0 and P25 under VIS irradiation, (b) samples pH0.5, pH0.7, pH1.0 and P25 under UV+VIS irradiation, (c) samples pH0.5–0.5, pH0.7–0.5, pH1.0–0.5 and P25 under VIS irradiation, and (d) samples pH0.5–0.5, pH0.7–0.5, pH1.0–0.5 and P25 under UV+VIS irradiation.

improving TiO_2 photocatalytic activity, ever since the pioneering work of Asahi et al.¹³ Up until now, a plethora of articles have been written, mainly focusing on anatase doping. Rutile is, in general, considered to be a less active species, so that the lack of papers on rutile doping is not surprising. Yet, as above mentioned, this was not the case with our samples (see section 3.1), where rutile was shown to be the more active phase. The experiments described in the following section were all prepared using the synthesis parameters that yielded the most active photocatalyst without doping, i.e. samples pH0.5–0.5 and pH0.7–0.5. In the present work three different dopants were considered as potential sources of nitrogen for doping, i.e. ammonium nitrate, urea, and tripropylamine. The dopants were added in different concentrations and at different pH values of the reaction mixtures (see section 2.1 for details).

3. 2. 1. Photocatalytic Properties of the Nitrogen Doped Samples, Using Urea, Ammonium Nitrate and Tripropylamine as Dopants

A pre-calculated amount of either urea or ammonium nitrate water solution was added to the reaction mixture before hydrothermal treatment, which was equivalent to 0.5, 1.0 or 2.0 at.% (normalized on oxygen at.%) of ni-

trogen doping. Tripropylamine was added in its pure form directly to the reaction mixture, which was equivalent to 0.5, 1.0 and 2.0 at.% of nitrogen doping. The pH of the reaction mixture was adjusted to either 0.5 or 0.7.

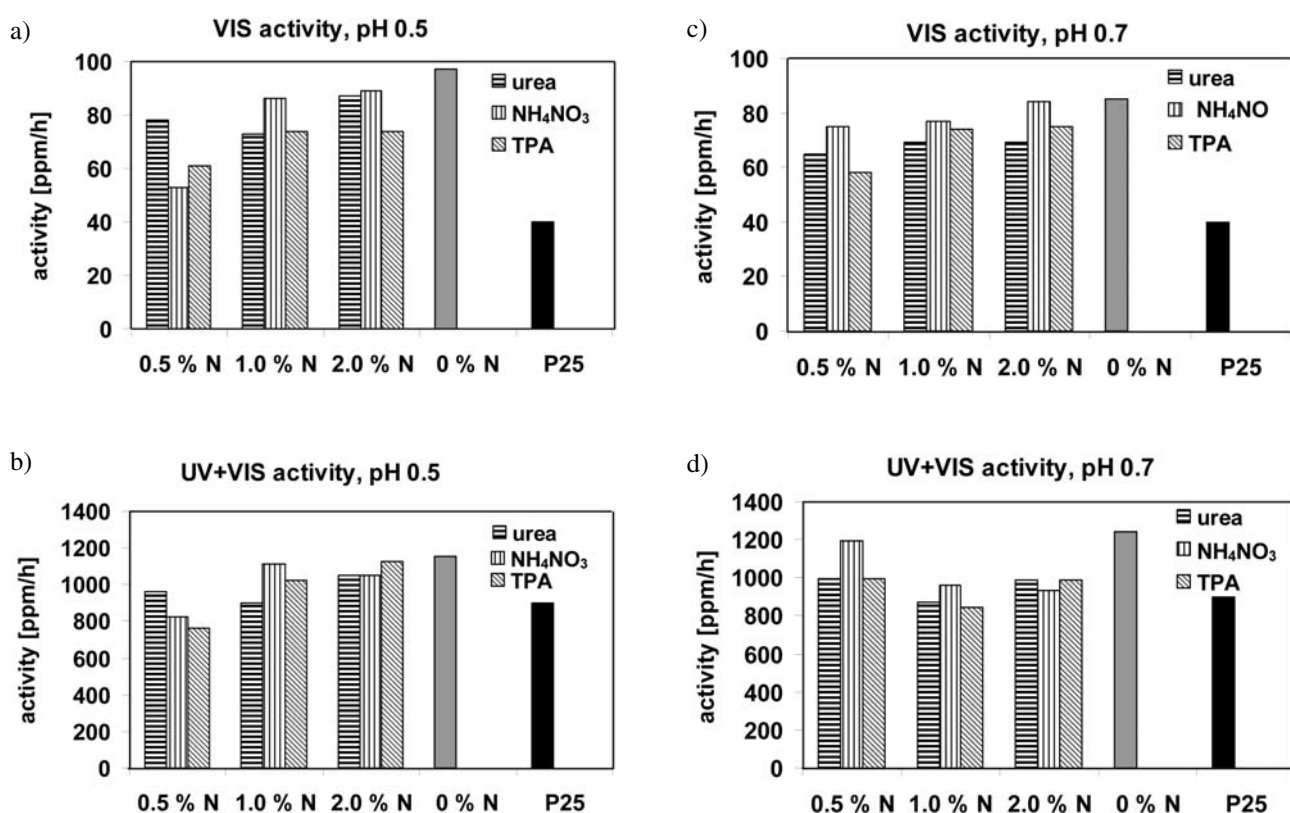
The XRD results showed that the doped samples at pH 0.5 and with the addition of isopropanol were predominantly in the rutile phase. The samples at pH 0.7 doped with ammonium nitrate at 0.5 at.% N and 1 at.% N contained a small fraction of the anatase phase, which made up 7 wt.% and 6 wt.% of the samples. Similarly, the samples doped with urea with 0.5 at.% and 1.0 at.% N doping at pH 0.7 both contained 5 wt.% of the anatase phase. All the other samples were composed of pure rutile.

BET specific surface was the lowest in the case of the sample with 2 at.% N doping, using NH_4NO_3 as a dopant, where it reached 44 m^2/g . The specific surface area of other solely rutile-containing samples ranged between 49 and 59 m^2/g . The samples containing a small amount of the anatase phase showed a somewhat higher BET specific surface area, which varied between 63 and up to 67 m^2/g . The data concerning structural analysis and BET specific surface area measurements of the doped samples are listed in Table 2.

As can be seen from Figure 7a–d, in all cases the nitrogen doping had a detrimental effect on the photocatalytic activity of the synthesized samples. There were, howe-

Table 2. The results of structural analysis and BET specific surface area measurements of the doped samples

Doping agent	N [at. %]	Anatase [wt. %]	pH = 0.5		BET SSA [m ² /g]	pH = 0.7		BET SSA [m ² /g]
			Rutile [wt. %]	Anatase [wt. %]		Rutile [wt. %]		
NH ₄ NO ₃	0.5	0	100	7	55	93	63	
NH ₄ NO ₃	1.0	0	100	6	51	94	67	
NH ₄ NO ₃	2.0	0	100	0	44	100	49	
Urea	0.5	0	100	5	54	95	60	
Urea	1.0	0	100	5	49	95	65	
Urea	2.0	0	100	0	48	100	53	
TPA	0.5	0	100	0	51	100	59	
TPA	1.0	0	100	0	54	100	54	
TPA	2.0	0	100	0	54	100	52	

**Figure 7.** Photocatalytic activity of the doped samples with different amounts of doping using different sources of nitrogen under (a) VIS irradiation, sample pH adjusted to 0.5, (b) UV+VIS irradiation, sample pH adjusted to 0.5, (c) VIS irradiation, sample pH adjusted to 0.7, and (d) UV+VIS irradiation, sample pH adjusted to 0.7.

ver, differences concerning the severity of the negative doping effect.

N doping, using urea as a nitrogen source, diminished photocatalytic activity at pH 0.5 with 1 at.% nitrogen loading. The smallest negative effect of urea doping was observed in the case of a 2 at.% nitrogen load. 0.5 at.% doping lies somewhere in between (Figure 7a, b). A similar observation can be made in the case of urea doping at pH 0.7 under UV+VIS irradiation (Figure 7d). At pH 0.7 un-

der VIS irradiation, 0.5 at.% N doping turns out to have the strongest negative effect (Figure 7c). 1 at.% and 2 at.% at pH 0.7 showed similar photocatalytic activity under VIS irradiation.

Where ammonium nitrate was used as a nitrogen source, N doping was most detrimental in the case of 0.5 at.% doping under VIS irradiation, which is true for the samples prepared at pH 0.5 and pH 0.7. Increasing nitrogen content also increased the photocatalytic acti-

vity. Still, even the most strongly doped sample, with 2 at.% N, did not reach the activity of the undoped sample (Figures 7a and c). The results are mixed under UV+VIS activity. At pH 0.5 1 at.% doping yielded the sample with the highest activity, whereas 0.5 at.% doping yielded the sample with the lowest activity (Figure 7b). On the other hand, at pH 0.7, the least doped sample showed the highest activity and an increasing nitrogen load only further diminished the photocatalytic activity (Figure 7d).

Under VIS irradiation, N doping using tripropylamine as nitrogen source had the most significant negative effect in the case of a 0.5 at.% nitrogen load. Increasing the nitrogen content also increased the photocatalytic activity of the samples at both pH 0.5 and 0.7. The same observation can be made for the samples at pH 0.5 under UV+VIS irradiation (Figure 7a–c). However, under UV+VIS irradiation the samples at pH 0.7 did not follow such a trend. The least doped sample was the most active, the second best is 2 at.% doping, and the least active sample was doped with 1 at.%.

None of the doped samples reached the photocatalytic activity of the undoped samples, neither at pH 0.5 nor at 0.7. Nitrogen doping, in general, therefore had a negative effect on photocatalytic activity. All the samples were more active than P25 under VIS irradiation, whereas under UV+VIS irradiation the signal was mixed, and differences were smaller.

3. 2. 2. The UV-VIS Diffuse Reflectance Spectra

The UV-VIS diffuse reflectance spectra of the samples doped with different sources of nitrogen were obtained. All the samples were doped with 2% N, and were prepared at a pH value of 0.5. The P25 industrial benchmark and the undoped sample pH0.5–0.5 were also included for comparison purposes.

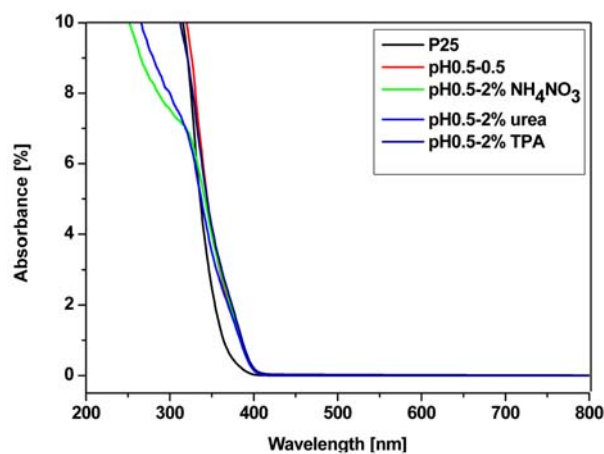


Figure 8. DRS analysis of samples P25, pH0.5–0.5, pH0.5–2% NH_4NO_3 , pH0.5–2% urea, and pH0.5–2% TPA.

The results of the DRS analysis are shown in Figure 8.

The DRS spectra showed that P25 has a lower absorption edge. This is not surprising, since the prevailing phase of P25 is anatase, which has a band gap of 3.2 eV. On the other hand all the other samples shown in Figure 8 are composed entirely of the rutile phase, which has a band gap of 3.0 eV. What is interesting is that there is no shift in the absorption edge of the doped samples in comparison with the undoped sample. No red shift, i.e. any reduction in the band gap energy, nor any blue shift, as has been proposed for nitrogen doped rutile by Di Valentin et al.¹⁴, was observed. Band gap shifting cannot be an appropriate explanation for the difference in the photocatalytic activity of the doped samples.

3. 2. 3. The FT-IR Spectra of the Synthesised Materials

FT-IR spectroscopy analysis was performed on an undoped sample and on several samples that had been doped with the highest amount of nitrogen, 2 at.%, using different sources of nitrogen for doping (see Figure 9).

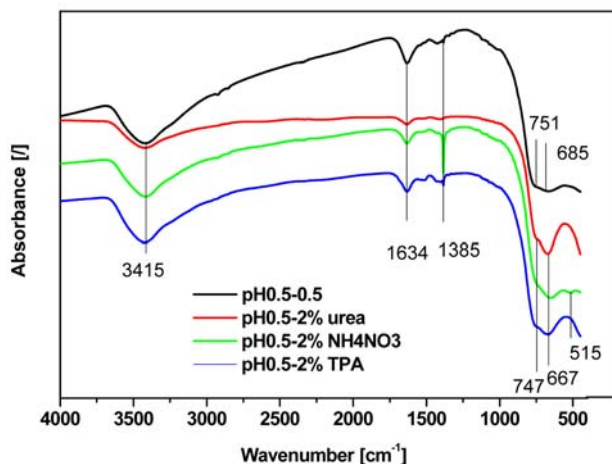


Figure 9. FT-IR spectra for the samples pH0.5–0.5, pH0.5–2% NH_4NO_3 , pH0.5–2% urea, and pH0.5–2% TPA.

By comparing the non-doped sample with those containing nitrogen, a slight shift towards a lower wavenumber can be seen in the low-frequency area, i.e. a shift from 685 cm^{-1} in the non-doped sample to 667 cm^{-1} , and a shift from 751 cm^{-1} to 747 cm^{-1} . There is also a new peak at 515 cm^{-1} in the sample doped with ammonium nitrate. The broad peak region from 400 to 1000 cm^{-1} is caused by a Ti-O stretch.¹⁶ Although a peak at 1385 cm^{-1} is present in all the samples, it is much more pronounced in the case of the sample that was doped with ammonium nitrate as

nitrogen source. It is barely noticeable in the urea doped sample and the undoped sample. This peak was attributed, by Xing et al.,³² to surface adsorbed NH_4^+ species. The absorption peak at 1634 cm^{-1} is characteristic of adsorbed H_2O , as reported by Nolan et al.¹⁶ The broad peak in the high frequency region at 3415 cm^{-1} was attributed, by Li et al.¹¹, to the OH species on the titania surface. This peak is most noticeable in the undoped sample and a large population of surface OH species might have contributed to its relatively high activity. Although, there are differences in the spectra of the analysed samples, overall, FT-IR analysis did not provide any definitive proof about the successful doping of nitrogen atoms in the TiO_2 crystal lattice. What can be said is that the surface OH group population is much higher in the case of the undoped sample, which may have contributed to its relatively high photocatalytic activity.

4. Conclusions

The hydrothermal synthesis method and titanium oxysulphate as the titanium source were used in order to produce photocatalytically active titania nanoparticles. The influence of pH, which varied between 0.5 and 1.0, was observed on product properties, as well as that of the addition of isopropanol. The results showed that a lower pH favours rutile formation. Isopropanol addition additionally favours crystallization of the rutile phase, and also boosts photocatalytic activity. The exact role of isopropanol during hydrothermal treatment is yet unknown. Rutile crystallizes in the form of a nanorod-like structure, 50–150 nm in length and 30–60 nm in width. On the other hand, anatase is composed of smaller spherical particles, 10–15 nm in diameter. The XRD and FE-SEM results were supported by the BET specific surface area measurements. A rutile specific surface area was measured at $43\text{--}58\text{ m}^2/\text{g}$, whereas results of more than $100\text{ m}^2/\text{g}$ were obtained in the case of the anatase-containing samples. Contrary to the findings in the literature, but not all of it,³³ it was observed that the rutile phase is the more active species, both under VIS and UV+VIS irradiation. Comparing our best sample with P25, ours was more than twice as active under VIS irradiation and significantly more active under UV+VIS irradiation (a factor of about 1.4). The attempted nitrogen doping did not result in samples with a higher photocatalytic activity. In fact, in the case of our samples doping seems to have diminished their photocatalytic activity. However, no clear relationship was found between the doping concentration and/or the doping source and diminished photocatalytic activity. No band gap shifting was observed in the doped samples. There were differences in the FT-IR spectra – the undoped sample had a higher concentration of surface OH groups compared to the doped samples, which may have contributed to its higher activity.

5. References

1. A. Fujishima, K. Honda, *Nature*. **1972**, *238*, 37–38.
2. O. Carp, C. L. Huisman, A. Reller, *Prog. Solid State Chem.* **2004**, *32*, 33–177.
3. S. Rehman, R. Ullah, A. M. Butt, N. D. Gohar, *J. Hazard. Mater.* **2009**, *170*, 560–569.
4. X. Chen, S. S. Mao, *Chem. Rev.* **2007**, *107*, 2891–2959.
5. A. Fujishima, K. Honda, T. Watanabe, *TiO₂ photocatalysis: fundamentals and applications*. 1997, Tokyo: BLC Inc.
6. M. D. Hernandez-Alonso, F. Fresno, S. Suarez, J. M. Coronado, *Energy Environ. Sci.* **2009**, *2*, 1231–1257.
7. S. Livraghi, M. Pelaez, J. Biedrzycki, I. Corazzari, E. Giamello, D. D. Dionysiou, *Catal. Today*, **2013**, *209*, 54–59.
8. T. Umebayashi, T. Yamaki, H. Itoh, K. Asai, *J. Phys. Chem. Solids*, **2002**, *63*, 1909–1920.
9. C. Di Valentin, G. Pacchioni, *Catal. Today*, **2013**, *206*, 12–18.
10. Y. Nosaka, M. Matsushita, J. Nishino, A. Y. Nosaka, *Sci. Technol. Adv. Mater.* **2005**, *6*, 143–148.
11. H. X. Li, J. X. Li, Y. I. Huo, *J. Phys. Chem.* **2006**, *110*, 1559–1565.
12. A. Fujishima, X. Zhang, D. A. Tryk, *Surf. Sci. Rep.*, **2008**, *63*, 515–582.
13. R. Asahi, T. Morikawa, T. Ohwaki, K. Aoki, Y. Taga, *Science*, **2001**, *293*, 269–271.
14. C. Di Valentin, E. Finazzi, G. Pacchioni, A. Selloni, S. Livraghi, M. C. Paganini, E. Giamello, *Chem. Phys.*, **2007**, *339*, 44–56.
15. S. Z. Chen, P. Y. Zhang, D. M. Zhuang, W. P. Zhu, *Catal. Commun.* **2004**, *5*, 677–680.
16. N. T. Nolan, D. W. Synnott, M. K. Seery, S. J. Hinder, A. Van Wassenhoven, S. C. Pillai, *J. Hazard. Mater.* **2012**, *211*, 88–94.
17. S. A. Wang, J. M. Xu, H. L. Ding, S. S. Pan, Y. X. Zhang, G. H. Li, *Crystengcomm*, **2012**, *14*, 7672–7679.
18. V. Etacheri, M. K. Seery, S. J. Hinder, S. C. Pillai, *Chem. Mater.* **2010**, *22*, 3843–3853.
19. N. Kometani, A. Fujita, Y. Yonezawa, *J. Mater. Sci.*, **2008**, *43*, 2492–2498.
20. S. M. Gupta, M. Tripathi, *Cent. Eur. J. Chem.* **2012**, *10*, 279–294.
21. X. B. Chen, S. S. Mao, *J. Nanosci. Nanotechnol.* **2006**, *6*, 906–925.
22. Y. V. Kolen'ko, A. A. Burukhin, B. R. Churagulov, N. N. Oleynikov, *Mater. Lett.* **2003**, *57*, 1124–1129.
23. Y. V. Kolen'ko, A. A. Burukhin, B. R. Churagulov, N. N. Oleinikov, *Inorg. Mater.* **2004**, *40*, 822–828.
24. K. Namratha, K. Byrappa, *Prog. Cryst. Growth Charact. Mater.* **2012**, *58*, 14–42.
25. K. Namratha, K. Byrappa, *J. Supercrit. Fluids*, **2013**, *79*, 251–260.
26. R. A. Spurr, H. Myers, *Anal. Chem.* **1957**, *29*, 760–762.
27. T. Marolt, A. Sever Škapin, J. Bernard, P. Živec, and M. Gaberšček, *Surf. Coat. Technol.* **2011**, *206*, 1355–1361.
28. J. Yang, S. Mei, J. M. F. Ferreira, *J. Am. Ceram. Soc.* **2000**, *83*, 1361–1368.

29. Y. M. Xu, X. M. Fang, J. A. Xiong, Z. G. Zhang, *Mater. Res. Bull.* **2010**, *45*, 799–804.
30. J. H. Yan, S. A. Feng, H. Q. Lu, J. A. Wang, J. F. Zheng, J. H. Zhao, L. Li, Z. P. Zhu, *Mater. Sci. Eng. B*, **2010**, *172*, 114–120.
31. G. Wang, *J. Mol. Catal. A: Chem.* **2007**, *274*, 185–191.
32. M. Y. Xing, J. L. Zhang, F. Chen, *Appl. Catal. B*, **2009**, *89*, 563–569.
33. J. Ryu, W. Choi, *Environ. Sci. Technol.* **2008**, *42*, 294–300.

Povzetek

S hidrotermalno metodo smo sintetizirali nanodelce titanovega oksida. Kot izvor titana smo uporabili TiOSO_4 . Spreminjali smo pH med 0,5 in 1,0 ter dodatek izopropanola v reakcijsko zmes in s tem pripravili različne zmesi anataza, rutila in brookita. Vzorce smo tudi dopirali z različnimi deleži dušika, pri čemer smo kot izvor dušika uporabili sečnino, amonijev nitrat in tripropilamin. Vzorce smo karakterizirali z rentgensko praškovo difrakcijo, elektronsko vrstično mikroskopijo na poljsko emisijo, infrardečo spektroskopijo, UV-Vis difuzno refleksijsko spektroskopijo in jim določali specifično površino. Fotokatalitsko aktivnost pa smo merili v reaktorskem sistemu plin-trdno. Ugotovili smo, da nizek pH favorizira nastajanje rutila, medtem ko višje vrednosti pH vodijo do mešanih polimorfnih faz titanovega oksida. Tudi dodatek izopropanola pospešuje nastajanje rutila. V nasprotju z večino literaturnih podatkov je bila v naši raziskavi najbolj fotokatalitsko aktivna rutilna modifikacija. Dopiranje z dušikom pa ne poveča fotokatalitske aktivnosti, ampak jo celo nekoliko zmanjša.